http://informahealthcare.com/xen
ISSN: 0049-8254 (print), 1366-5928 (electronic)

Xenobiotica

Xenobiotica, 2013; 43(7): 628–635
 DOI: 10.3109/00498254.2012.753490

informa healthcare

RESEARCH ARTICLE

Metabolite profile analysis of aconitine in rabbit stomach after oral administration by liquid chromatography/electrospray ionization/multiple-stage tandem mass spectrometry

Zhigang Sui[1,2], Na Li[2], Zhiqiang Liu[3], Jun Yan[1], and Zhongying Liu[1]

[1]*College of Pharmacy, Jilin University, Changchun, China,* [2]*Dalian Institute of Chemical Physics, Chinese Academy of Sciences, Dalian, China, and* [3]*Chang Chun Institute of Applied Chemistry, Chinese Academy of Sciences, Changchun, China*

Abstract

1. Aconitine (AC), an active and highly toxic constituent extracted from aconitum plants, is well known for its excellent effects against rheumatism and rheumatoid arthritis. The metabolism of AC in liver and intestine has been previously reported. However, little is known about the metabolism of AC in stomach. In this study, the metabolite profiling of AC in stomachs of rabbit and rat was performed by liquid chromatography/electrospray ionization/multiple-stage tandem mass spectrometry (LC/ESI/MS^n), for the first time.
2. The samples were purified by liquid–liquid extraction, separated using an Agilent extended C18 column following a linear gradient elution and then detected by ESI/MS^n in positive ion mode. Metabolites were identified by comparing their protonated molecules, fragmentation patterns and chromatographic behaviors with those of standard compounds and data from authorized literature works.
3. In conclusion, 14 metabolites were identified in animal stomach after oral administration of AC. The presentation of a large amount of metabolites of AC in stomach suggested that, for aconitum alkaloids, the stomach might play an important role in their metabolism.

Keywords

Aconitine, fragmentation pathway, LC/ESI/MS^n, metabolites, stomach

History

Received 19 September 2012
Revised 21 November 2012
Accepted 23 November 2012
Published online 26 December 2012

Introduction

In East Asia, there are some traditional aconitum plants (*Ranunculaceous* family), such as *Aconitum kusnezoffii* and *Aconitum brachypodum* (Singhuber et al., 2009), which are widely used for more than a dozen of centuries because of their analgetic and anti-inflammatory activities (Suzuki et al., 1994), especially the excellent effects against rheumatosis and rheumatoid arthritis. However, they also induce serious arrhythmias with final result leading to death (Turabekova et al., 2008). Some diester-diterpene alkaloids, such as aconitine (AC), mesaconitine, hypaconitine and deoxyaconitine, are considered to be the main, active and toxic constituents (Yue et al., 2009) and share a common C_{19}-norditerpenoid skeleton (Wang et al., 2003). Every year, fatal cases of poisoning from aconitum plants are reported (Pullela et al., 2008; Strzelecki et al., 2010) due to the narrow therapeutic index of aconitum alkaloids (Li et al., 2012). It is reported that the median lethal dose of AC for mice (iv) is 0.270 ± 0.002 mg/kg (Zhou et al., 1984), and its lethal dose for humans is estimated to be 1–2 mg (single dose). On the other hand, aconitum alkaloids are unstable and undergo rapid biotransformation *in vivo* (Zhang et al., 2005), which result in the production of new metabolites with different levels of toxicity or detoxificated metabolites. Therefore, the investigation on metabolism of AC, the representative aconitum alkaloid, is valuable for the toxicological, pharmacological and clinical research of aconitum plants.

In general, the unprocessed aconitum herbs are too toxic for internal use, but they can be used for external application as anesthetics (Singhuber et al., 2009). The processed aconitum herbs are commonly administrated via oral route in the formulations of decoction or medicinal wine (Chan, 2011). Liver is the main site of drug metabolism, where cytochrome P450 enzymes are significant phase-I drug metabolizing enzymes involved in the metabolism of drugs. Several literature works on metabolism of AC in liver microsomes are available and several metabolites have been identified (Tang et al., 2011; Wang et al., 2006). Because patients are given aconitum herbs predominantly via oral administration, AC, the main active compound in the herbs, will unavoidably undergo biotransformation in alimentary canal, which contains numerous microorganisms and diverse enzymes, such as trypsin, chymotrypsin, elastase and carboxypeptidases (Sarti et al., 2011), and produce metabolites. Our previous study has found some metabolites in small

Address for correspondence: Zhongying Liu, College of Pharmacy, Jilin University, 1266 FuJin Road, Changchun 130021, China. Tel: +86 431 85619704. Fax: +86 431 85262236. E-mail: Liuzy@jlu.edu.cn

intestine, cecum and rectum (Sui et al., 2009). However, there has been no report about the metabolite profiling of AC in the stomach. Compared with the intestine, the stomach is usually believed to have minimal contribution to metabolism and typically make a much more important contribution to dissolution and absorption of drugs. Therefore, the biotransformation of drugs in the stomach is usually ignored. However, the endogenous factors (e.g. pepsin and bacteria) in the stomach may also have effect on drug metabolism (Delgado et al., 2011; Gupta et al., 2012). For example, arctiin has been reported to be transformed into arctigenin in rat stomach, where the concentration of arctigenin was significantly higher than that of arctiin (He et al., 2012). Zhang et al. (2008) found that polydatin could be transformed into resveratrol by de-sugaring process in rat stomach. In addition, baicalin, the main metabolite of baicalein, could be detected in rat stomach 20 min after oral administration of baicalein and maintained at a stable concentration for at least 16 h (Liu et al., 2009). Herein, we focused on the biotransformation of AC in the stomach, the first site of metabolism in the alimentary canal.

Owing to the high toxicity, AC should be orally administered with low dose, which causes low concentrations of AC and its metabolites in the biological samples. Therefore, it is necessary to choose a sensitive and specific analytical method. Liquid chromatography/electrospray ionization/multiple-stage tandem mass spectrometry (LC/ESI/MS^n) can meet the above-mentioned requirements and has been widely used in pharmaceutical research, especially in studies of drug metabolism. Because AC-type alkaloids have a strong gaseous basicity and proton affinity, they are also suitable for ESI/MS^n analysis.

In this study, LC/ESI/MS^n in positive ion mode was used to elucidate and identify the metabolites of AC. To investigate the metabolism of AC sufficiently, rat and rabbit were chosen as the model animals. To determine if the acid environment in stomach will ''metabolize'' the AC, comparative data of AC incubated in acidic solution were also provided. Totally, 14 metabolites were unambiguously identified or tentatively deduced by comparing their protonated molecules, fragmentation pathways and chromatographic behaviors with those of standard compounds and reports in literature works. The elemental compositions of some product ions were also analyzed by Fourier transform ion cyclotron resonance mass spectrometry (FT-ICR-MS). Finally, a biotransformation pathway of AC in the stomach was proposed.

Materials and methods

Chemicals and reagents

The standard compounds, AC, mesaconitine and hypaconitine (purity >99%), were purchased from the National Institute for the Control of Pharmaceutical and Biological Products (Beijing, China). Methanol, acetonitrile and acetic acid were of HPLC grade and were purchased from Thermo Fisher Scientific, Inc. (Waltham, MA). Purified water was produced using a Milli-Q ultra-pure water system (Billerica, MA). All other reagents and chemicals were of analytical grade.

Table 1. The LC gradient program.

Time (min)	Flow (mL/min)	A (%)	B (%)	C (%)
0	0.6	35	65	0
30	0.6	80	20	0
60	0.6	90	10	0
120	0.6	0	0	100

Apparatus and operation conditions

The high-performance LC system consisted of a Waters 996 photo-diode array detector and a Waters 2695 HPLC (Milford, PA) equipped with a Millennium 32 software program (Milford, PA) for data analysis. Separation of the components was performed on an Agilent extend C_{18} column ($4.6 \times 150\,mm^2$, 5 μm; Agilent Technologies Inc, Santa Clara, CA) with a column temperature of 30 °C. The mobile phase (Table 1) consisted of mixed organic phase (A), water phase (B) and pure methanol phase (C). Elution solvent A consisted of 50% methanol and 50% acetonitrile, and elution solvent B consisted of 0.2% acetic acid and 2% ammonia, which was adjusted to the desired pH value (10.50) using ammonia solution (1%, v/v). The mobile phase flow rate was 0.6 mL/min. Just before the eluent entered the MS, its flow rate was reduced to 0.3 mL/min by a split-flow valve.

MS was performed on a LCQ ion trap mass spectrometer (Finnigan, San Jose, CA) with an electrospray source. The spraying voltage was set at 5.00 kV, the tube voltage at 15 V, the capillary voltage at 17 V and the capillary temperature at 200 °C. The LC fluid was nebulized using high-purity nitrogen (N_2). The sheath gas and auxiliary gas flow rates were set at 60 and 10 arbitrary units, respectively. The collision gas used for MS^n was helium (He). The collision energies (%) ranged from 25% to 40%, and the isolation width was 1.5 mass units. Data were collected and analyzed by Xcalibur software (version 1.0; Thermo Fisher Scientific, San Jose, CA). The high resolution mass data were obtained on an Ionspec 7.0 T FT-ICR-MS (Ionspec Corporation, Irvine, CA) with a Z-spray electrospray source. Negative-ion mass spectra were acquired after the solutions were directly infused into the source region with a flow rate of 3.0 μL/min. The parameters were set as follows: the source temperature 80 °C, probe temperature 100 °C, sample cone voltage 30 V, extractor cone voltage 5 V, probe high voltage 3.5 kV, desolvation gas voltage 0.1 V and cone gas voltage 0.85 V. The spectrum was scanned from *m/z* 108 to 1000 at 1024 K data points, with an ADC rate of 2 MHz.

As the concentrations of different metabolites varied significantly, the metabolites at low concentrations can only generate small peaks in the ion chromatogram, resulting in too little time for MS^n analysis. To solve this problem, a channel-switching technique was applied to enrich the metabolites at low concentrations. In the interface between LC and MS, a six-port switch was installed. This device has been commonly used to reduce the flow rate of eluate from LC to make it suitable for MS. Furthermore, it can also be used to enrich the metabolites which are of low abundance and unable to be analyzed online by MS^n analysis. The total ion chromatogram of certain sample, showing the retention time and peak width of the ion peak of each metabolite, was

first obtained in full scan mode. Subsequently, the same sample was injected for the second time into the LC/MS system for MS^n analysis. Utilizing the channel switch, the metabolites at low concentrations in the eluate were collected. The start time and collection duration of each metabolite depended on its retention time and peak width. After being concentrated by nitrogen stream, the collected sample was injected to MS spectrometer at 3 μL/min by a syringe pump. If the metabolite concentration in the eluate was still not high enough, the enrichment process could be performed repeatedly.

Animal experiment and sample preparation

The animal protocol was approved by the Jilin University Animal Ethics Committee. Ten rabbits (six months, 2500 ± 50 g) and 10 rats (four weeks, 200 ± 20 g) were purchased from the Laboratory Animal Center of Jilin University (Changchun, China) and were housed individually in a room with a controlled temperature (22 ± 1 °C) and humidity ($60 \pm 5\%$), 12 h dark/light cycle for one week before the experiments. The rabbits and rats were divided into two equal groups ($n = 5$), respectively, and fasted for 12 h prior to use, but had free access to water. The animals in the dosed group were orally administered with aqueous suspension of AC (0.5 mg/kg), while the animals in the control group were orally administered with only water. It is reported that the half value period of AC in rabbits is 56 min after administration (Wang et al., 2004). In this study, for the sake of producing more metabolites, the time of sacrifice was set at 4 h, 4 times longer than the half value period. The endogastric contents were collected immediately after sacrifice and stored at −80 °C until analysis.

Five grams of endogastric contents were diluted with 20 mL of water and shaken for 60 s. Then, the suspension was centrifuged at 4000 r/min for 10 min. After centrifugation, the upper layer was separated and collected, 20 mL of ethyl acetate was added and the resulting solution was shaken for 5 min. Then, the mixed solution was centrifuged at 4000 r/min for 10 min. After extraction, the upper phase was evaporated to dryness under a stream of nitrogen gas at 30 °C, and the residue was dissolved in 0.5 mL of acetonitrile. The solution was finally passed through a 0.45 μm nylon membrane, and an aliquot of 10 μL filtrate was injected into the $LC/ESI/MS^n$ system for analysis.

The acid solution was prepared according to the simulated gastric fluid with modification (Consolini et al., 2012). In brief, 1 mL of acid solution contained 0.084 N HCl and 35 mM NaCl, with pH1.2. 20 mL of 1 mM AC were prepared in acid solution and supplemented with 10 mg of standard oleic and stearic acid, and then placed in a 37 °C shaking water bath for 4 h. Then, the incubated samples (20 mL) were collected and processed following the same protocol of endogastric contents for further analysis.

Results and discussion

Most metabolites have structural similarities to the parent drug, and this may yield common fragmentation pathways. Therefore, it is logical to use the fragmentation pathways of parent drugs to identify the structures of their potential metabolites. To obtain more extensive and detailed mass spectral patterns of AC, two of its analogs, mesaconitine and hypoconitine, were analyzed as well. The structures of AC and its analogs are presented in Table 2.

Table 2. The structures of AC and its analogs.

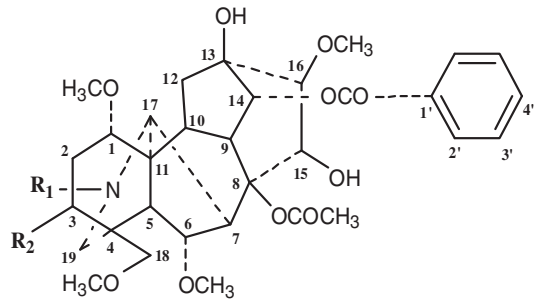

Alkaloids	R_1	R_2	MW
AC	C_2H_5	OH	645
Mesaconitine	CH_3	OH	631
Hypaconitine	CH_3	H	615
Deoxyaconitine	C_2H_5	H	629

$LC/ESI/MS^n$ analysis of aconitine, mesaconitine and hypaconitine

Prior to analysis, the LC and MS conditions were optimized to improve separation efficiency and signal strength, and the $LC/ESI/MS^n$ method was performed to determine the retention time and obtain mass spectral data for the standard compounds. The LC chromatogram of standard compounds is shown in Supplementary Figure 1.

AC eluted at 47.6 min and yielded a $[M + H]^+$ at *m/z* 646. The base peak in the MS^2 spectrum, $[M + H - 60]^+$, appeared at *m/z* 586, corresponding to the elimination of acetic acid formed by the C_8-acetyl group. The absence of the $[M + H - 60]^+$ from the MS^2 spectrum of an AC metabolite indicates that it does not possess C_8 acetyl. The base peak in the MS^3 spectrum of AC, $[M + H - 60 - 32 - 28]^+$, appeared at *m/z* 526, corresponding to the combined loss of CO and methanol. The literature has shown that the hydroxyl of C_{15} plays a key role in this process (Wang et al., 2002). Detection of the $[M + H - 60 - 32 - 28]^+$ in the MS^3 spectrum of an AC metabolite indicates that it has the C_{15} hydroxyl group. In the MS^4 spectrum of the $[M + H - 60 - 32 - 28]^+$, a product ion $[M + H - 60 - 32 - 28 - 122]^+$ could be found at *m/z* 404, corresponding to the loss of benzoic acid produced by C_{14} benzoyl group. The MS^n spectra of AC, mesaconitine and hypaconitine are shown in Supplementary Figure 2.

Compared with AC, mesaconitine and hypaconitine also produce product ions arising from successive neutral losses of acetic acid, methanol, CO and benzoic acid. Of course, the mass of these product ions will shift depending on the difference between their molecular weight and that of AC. It is clear that the fragmentation mechanisms of these three compounds display common patterns because of their similar structures. However, comparison of the MS^2 spectra of AC, mesaconitine and hypaconitine reveals a special ion $[M + H - 18]^+$. This product ion with low intensity could

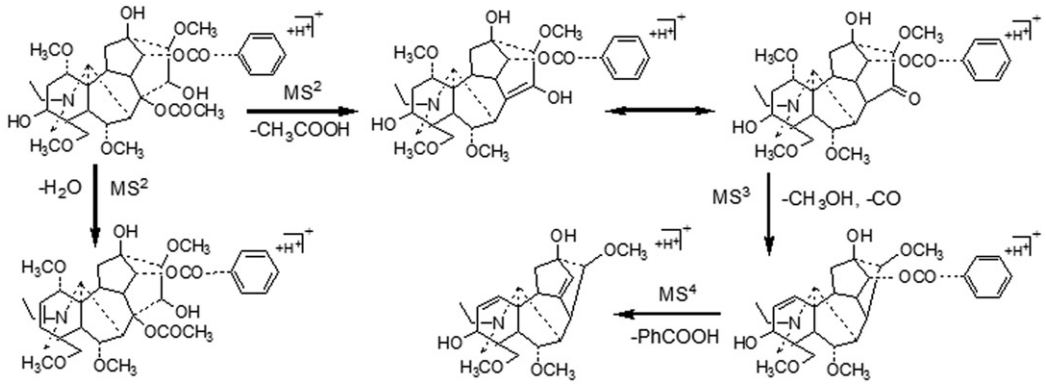

Figure 1. The main fragmentation pathways of AC.

be detected in the spectra of AC (*m/z* 628) and mesaconitine (*m/z* 614), but not in the spectrum of hypaconitine. AC and mesaconitine possess a C_3 hydroxyl group, whereas hypaconitine does not, linking detection of the $[M+H-18]^+$ to the presence of C_3 hydroxyl group. Therefore, if the $[M+H-18]^+$ were detected in the MS^2 spectrum of an AC metabolite, the C_3 hydroxyl group should exist in that metabolite.

The fragmentation pathways of AC contain some special ions, called diagnostic ions, which indicate the presence of specific groups. On the contrary, the absence of such diagnostic ions indicates that the corresponding groups do not exist. Four diagnostic ions, $[M+H-18]^+$, $[M+H-60]^+$, $[M+H-60-32-28]^+$ and $[M+H-60-32-28-122]^+$ were found in this study. The detection of these ions are related to the C_3 hydroxyl, C_8 acetyl, C_{15} hydroxyl and C_{14} benzoyl group, respectively, and play an important role in the identification of metabolites of AC. The main fragmentation pathways of AC are shown in Figure 1.

Identification of hydrolysis products of AC in acid solution

The base peak ion chromatogram for LC/MS analysis of an incubation of 1 mM AC with standard fatty acid in acid solution is shown in Supplementary Figure 3. The peak eluting at 49.1 min displayed the $[M+H]^+$ at *m/z* 646 and corresponded to unmodified AC. The MS^2 and MS^3 spectra of the $[M+H-60]^+$ provided a number of product ions, such as ions at *m/z* 586, 526 and 404, which are characteristic fragment ions of AC.

Except unchanged AC, two hydrolysis products were identified. H^1 eluted at 11.4 min and showed the $[M+H]^+$ at *m/z* 542, showing a loss of 104 Da (*m/z* $646 \rightarrow 542$) from AC. The MS^2 spectrum showed the dominant ion $[M+H-60]^+$ at *m/z* 482 while the MS^3 spectrum of $[M+H-60]^+$ generated a dominant ion at *m/z* 422. The two dominant ions were 104 Da lower than the corresponding ions (at *m/z* 586 and 526) of AC, respectively. Thus, the metabolite had a fragmentation mode similar to AC, indicating that their diterpenoid skeleton were intact. The reduction of 104 Da in molecular weight showed that H^1 was a debenzoylated metabolite of AC. The first loss of 60 Da (*m/z* $542 \rightarrow 482$) was proposed to arise via the loss of a neutral molecule of CH_3COOH. The second loss of 60 Da (*m/z* $482 \rightarrow 422$) was proposed to be due to the loss of neutral molecules of CH_3OH and CO. Thus, H^1 was identified to be 14-*o*-debenzoylaconitine. The retention time of H^2 was 20.6 min and the $[M+H]^+$ exhibited at *m/z* 604. The MS^2 spectrum displayed $[M+H-18-32]^+$ as the base peak at *m/z* 554. $[M+H-60]^+$ was not detected, suggesting that the C_8 acetyl does not exist in H^2. The 42 Da (*m/z* $646 \rightarrow 604$) decrease in molecular weight indicates that H^2 might be deacetylated from AC. The loss of 50 Da from the precursor ion (*m/z* $604 \rightarrow 554$) was proposed to arise via the combined loss of neutral molecules of CH_3OH and H_2O. Therefore, H^2 was deduced as 8-*o*-deacetylaconitine, also named benzoylaconitine. The MS^n spectra of H^1 and H^2 are shown in Supplementary Figure 4.

Identification of metabolites of AC in rabbit

For identifying the metabolites in rabbit stomach, the base peak ion chromatogram of the endogastric contents, obtained by LC/MS in full scan mode, is shown in Figure 2. Compared with the control, 14 metabolites of AC were detected except unchanged AC and its hydrolysis products. Each metabolite was identified on the basis of its retention time, mass spectra and fragmentation patterns generated by LC/ESI/MS^n analysis.

M^1, M^3 and M^6 had LC retention times of 12.5, 31.1 and 51.3 min, respectively. All of them showed $[M+H]^+$ at *m/z* 662 (data not shown), 16 Da (*m/z* $646 \rightarrow 662$) higher than AC, suggesting that they were isomers of oxidized metabolites of AC. For M^1 and M^3, their MS^2 spectra both contained $[M+H-60]^+$ as the base peak at *m/z* 602, and the MS^3 spectra of precursor ions $[M+H-60]^+$ both showed $[M+H-60-32-28]^+$ as the base peak at *m/z* 542. The base peaks of M^1 and M^3 were all 16 Da higher than that of AC in the corresponding spectra, indicating fragmentation patterns of M^1 and M^3 are similar to that of AC. In addition, the $[M+H-60-32-28-138]^+$ at *m/z* 404 was detected in their MS^3 spectra. Compared with the corresponding $[M+H-60-32-28-122]^+$ of AC (also at *m/z* 404), the $[M+H-60-32-28-138]^+$ suggested the occurrence of a hydroxylation reaction on the C_{14} group. Considering that there are three positions of hydroxylation on the benzene ring, the specific position is uncertain. However, the base peak in

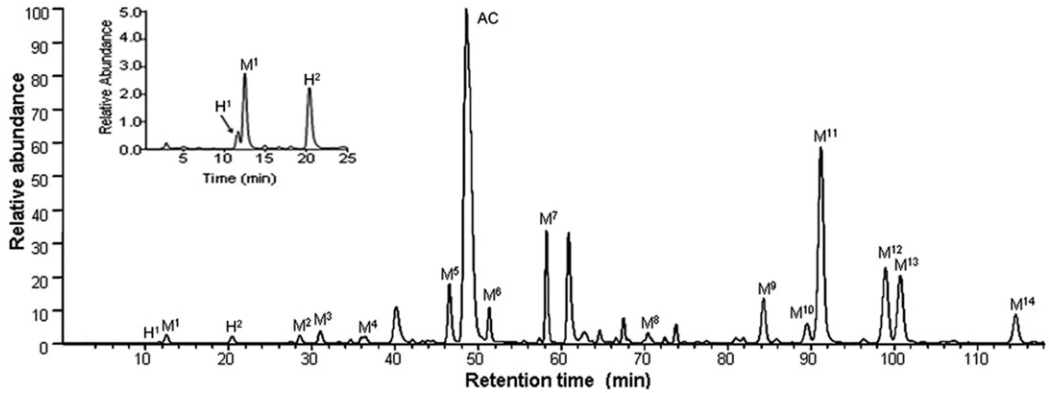

Figure 2. The base peak ion chromatogram of AC and its metabolites formed in rabbit stomach, as monitored by LC/MS.

the MS^2 spectrum of M^6 was detected at *m/z* 542, a loss of 120 Da (*m/z* 662 → 542) from the precursor ion. Through FT-ICR-MS analysis, the elemental composition of $C_7H_4O_2$ was obtained, and the unsaturation value was calculated to be 6. We deduced that the neutral loss must contain a benzene ring, which came from the C_{14} benzoyl. This never-before-reported fragmentation pathway is elucidated in Supplementary Figure 5, in which the hydroxylation occurs at the para-position of the benzene ring (C_4 position). Therefore, M^6 was identified as 4′-hydroxylaconitine, and M^1 and M^3 were deduced to be 2′-hydroxylaconitine or 3′-hydroxylaconitine. The LC–MS^n spectra of M^1, M^3 and M^6 are shown in Supplementary Figure 6.

M^4 eluted at 36.4 min and its MS^2 spectrum showed the $[M+H]^+$ at *m/z* 632, a loss of 14 Da (*m/z* 646 → 632) from AC. The MS^2 spectrum and MS^3 spectrum of M^4 exhibit similar patterns to those of AC. The data suggest that M^4 is a demethylated metabolite of AC. If the demethylation occurred on the ethyl group of the N atom, mesaconitine would be produced and the retention time would be 37.6 min. However, the retention time of M^4 was less than that of mesaconitine. Because the C_{16}, C_1, C_6 and C_{18} positions all possess methoxyl group, demethylation could occur at any of these positions, making the specific position uncertain. Therefore, M^4 was deduced to be demethylaconitine.

M^2 had a retention time of 28.7 min and showed the $[M+H]^+$ at *m/z* 618. The MS^2 spectrum of the $[M+H]^+$ generated a base peak at *m/z* 558, and the base peak of the MS^3 spectrum was detected at *m/z* 526. The protonated molecule of M^2 was 28 Da (*m/z* 646 → 618) lower than that of AC and was 14 Da lower than the protonated molecule of M^4, suggesting that M^2 was a further demethylated derivative of M^4 or a *N*-de-ethylated product of AC. Therefore, M^2 was identified as didemethylaconitine or *N*-de-ethylaconitine.

M^5 and M^7 had retention times of 46.5 and 58.2 min, respectively. Both of them exhibited protonated molecule at *m/z* 630, a reduction of 16 Da (*m/z* 646 → 632) from AC, suggesting they were isomers of dehydroxylated derivatives of AC. The difference between M^5 and M^7 lies in the position of dehydroxylation in AC. Hydroxyl group existed at positions C_3, C_{13} and C_{15}, suggesting dehydroxylation could occur at any of them. According to the fragmentation pathways discussed above, the $[M+H-18]^+$ is generated by the loss of water from the C_3 hydroxyl group, and the $[M+H-60-32-28]^+$ is generated only when the C_{15} hydroxyl group exists. Comparing the MS^n spectra of M^5 and M^7, the $[M+H-60-32-28]^+$ was not detected in the MS^3 spectrum of M^5, and the $[M+H-18]^+$ was not detected in the MS^2 spectrum of M^7. Hence, M^5 was identified to be indaconitine which lost the hydroxyl of C_{15}, and M^7 was identified as deoxyaconitine which lost the hydroxyl of C_3. The LC–MS^n spectra of M^4, M^2, M^5 and M^7 are shown in Supplementary Figure 7.

All AC-type alkaloids share a common C_{19}-norditerpenoid skeleton and they can be classified into several types according to the groups at the C_8 and C_{14} positions of the skeleton. When an AC-type alkaloid has a benzoyl group at the C_{14} position and a fatty acyl group at the C_8 position, it is called lipoaconitine. In this study, some metabolites of lipoalkaloid type were also detected. M^8 eluted with a retention time of 70.4 min and showed the $[M+H]^+$at *m/z* 978. The MS^2 spectrum contained a base peak at *m/z* 586, which was selected for the MS^3 analysis. Its MS^3 spectrum provided characteristic product ions at *m/z* 526 and 554, showing the same fragmentation pathway as that of the *m/z* 586 ion produced by AC. So, we can deduce that the two product ions at *m/z* 586 are the same ion. The only difference between M^8 and AC lies in the groups at the C_8 position. The loss of 392 Da (*m/z* 978 → 586) suggested that M^8 lost a hexacosandienoic acid from the C_8 position. Therefore, M^8 was identified as 8-hcdo-benzoylaconine. Here, ''hcdo'' represents the residue of hexacosandienoic acid. According to the characteristic fragmentation patterns of lipoaconitines, if a metabolite has a higher molecular weight than AC, its MS^2 spectrum shows main product ion at *m/z* 586 and the MS^3 spectrum of precursor ion (*m/z* 586) is identical to that of the $[M+H-60]^+$ derived from AC, it can be logically concluded to be a lipoaconitine. Once the fatty acids are identified, their structures can be elucidated. Then, other lipoaconitines can be identified according to the identification process of M^8. The MS^n spectra of these lipoaconitines are shown in Supplementary Figure 8.

Based on their chromatographic behaviors and MS^n data, all the metabolites in the rabbit endogastric contents were identified and are presented in Tables 3 and 4. Proposed metabolism pathways of AC are shown in Figure 3.

Table 3. Data from AC, its hydrolysis products (H^1 and H^2) and its metabolites (M^1–M^7).

Compound	T_R (min)	MS (*m/z*)	MS^2 (*m/z*)	MS^3 (*m/z*)	Identification
H^1	11.6	542	482	422	14-*O*-Debenzoylaconitine
M^1	12.5	662	602	542	2′-Hydroxylaconitine or 3′-Hydroxylaconitine
H^2	20.4	604	554	522	8-*O*-Deacetylaconitine
M^2	28.7	618	558	526	Didemethylaconitine or *N*-de-ethylaconitine
M^3	31.1	662	602	542	3′-Hydroxylaconitine or 2′-hydroxylaconitine
M^4	36.4	632	572	512	Demethylaconitine
M^5	46.5	630	570	520	Indaconitine
AC	48.2	646	586	526	Aconitine
M^6	51.3	662	542	482	4′-Hydroxylaconitine
M^7	58.2	630	570	510	Deoxyaconitine

Table 4. Data from AC's metabolites (M^8–M^{14}).

Compound	T_R (min)	Parent ion (*m/z*)	Neutral loss (Da)	Daughter ion (*m/z*)	Fatty acid	Identification
M^8	70.4	978	392	586	Hexacosandienoic (hcdo)	8-Hcdo-benzoylaconine
M^9	84.3	864	278	586	Linolenic (lin)	8-Lin-benzoylaconine
M^{10}	89.5	828	242	586	Pentadecanoic (pdo)	8-Pdo-benzoylaconine
M^{11}	91.2	866	280	586	Linoleic (lol)	8-Lol-benzoylaconine
M^{12}	98.9	842	256	586	Palmitic (pal)	8-Pal-benzoylaconine
M^{13}	100.7	868	282	586	Oleic (ole)	8-Ole-benzoylaconine
M^{14}	114.6	870	284	586	Stearic (ate)	8-Ste-benzoylaconine

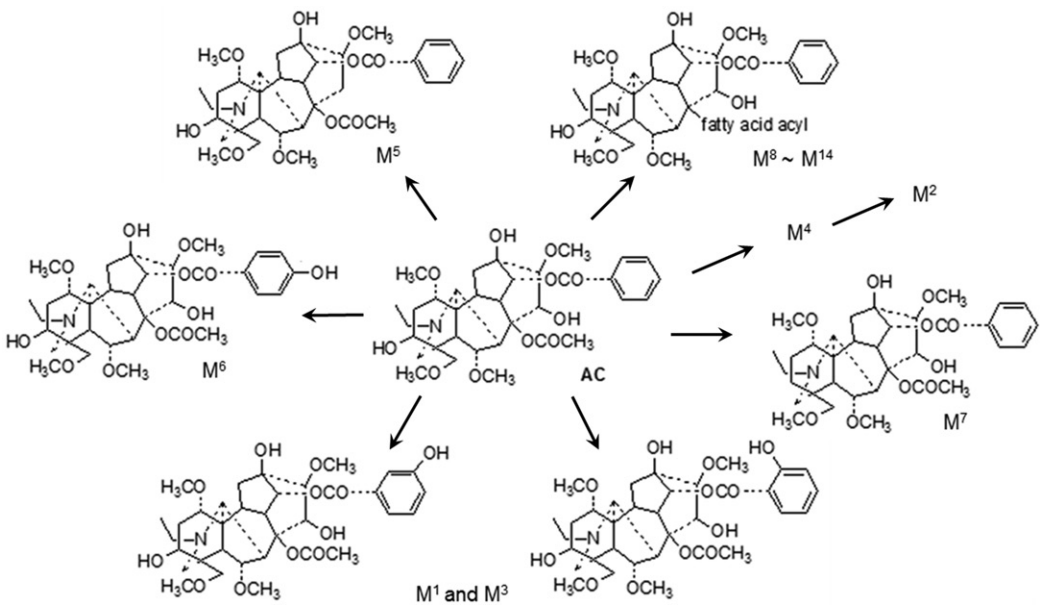

Figure 3. The proposed biotransformation process of AC in rabbit stomach.

Identification of metabolites of AC in rat

The base peak ion chromatogram of the endogastric contents of rat, obtained by LC/MS in full scan mode, is shown in Figure 4. Totally, 10 metabolites were detected compared with the control and all of them have been detected in endogastric contents of rabbit. The metabolite profiling of AC obtained from stomachs of rabbit and rat is very similar except that the metabolites in rat are fewer. All the metabolites in the rat endogastric contents were identified and are summarized in Supplementary Tables 1 and 2.

Up to now, some *in vivo*/*in vitro* studies have been reported on metabolism of AC in human and animal species. However, there has been no report available on the metabolism of AC in stomach, which is generally considered an organ with little contribution on drug metabolism. In this paper, we focused on investigating the metabolism of AC in stomach and found a total of 14 metabolites in the stomachs of rabbits and rats, indicating that the metabolism of AC dose exists in animal stomachs. Among these metabolites, didemethylaconitine or *N*-de-ethylaconitine (*m/z* at 618) and demethylaconitine (*m/z* at 632) have been detected in human liver microsomes

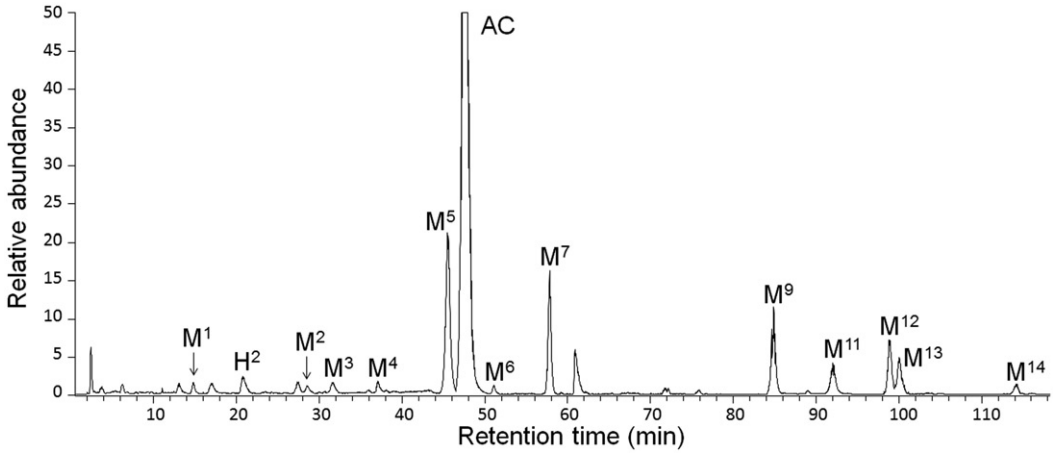

Figure 4. The base peak ion chromatogram of AC and its metabolites formed in rat stomach, as monitored by LC/MS.

(HLMs) (Tang et al., 2011; Wang et al., 2006). Three isomers of hydroxylaconitine (*m/z* at 662) and their deduced structures are reported in the present study for the first time. Although one isomer of hydroxylaconitine has been detected in HLMs by Tang et al. (2011), the exact position of hydroxylation was not been clarified. For the two metabolites at *m/z* 630, deoxyaconitine has been identified when AC was incubated with human intestinal bacteria *in vitro* (Zhao et al., 2007) while indaconitine was firstly reported to be transformed from AC in this work. With regard to the identified lipoaconitines, most of them have been detected previously in human intestinal bacteria incubation system except for 8-hcdo-benzoylaconine and 8-lin-benzoylaconine (Zhao et al., 2008). Meanwhile, for the two hydrolyzates, 8-*O*-deacetylaconitine (*m/z* at 604) was reported by many previous studies (Kentaro et al., 2005; Zhang et al., 2005) whereas 14-*O*-debenzoylaconitine (*m/z* at 542) was scarcely mentioned.

It is generally considered that few metabolites would be produced in stomach for its minimal contribution to metabolism. However, for AC, its metabolites found in stomachs of animals (rats and rabbits) are abundant. This indicates that the stomach, commonly considered a digestive organ, also plays an important role in metabolism of some compounds, such as diterpenoid alkaloids. Maybe it is because that some components in stomach, such as gastric enzymes, can catalyze the transformation of AC. In addition, it was reported that AC could be metabolized into some lipoaconitines by incubation with intestinal bacteria (Zhao et al., 2008), suggesting that the bacteria in stomach may also play a role in the metabolism of AC.

It is reported that lipoaconitines and monoester ACs have lower toxicity than AC (Wang et al., 2003), so do indaconitine and deoxyaconitine. Furthermore, lipoalkaloids are reported to have obvious anti-inflammatory effect, which is significantly influenced by the grade of unsaturation and length of the fatty acid chain (Borcsa et al., 2011). Therefore, the metabolism of AC in stomach can change its intrinsic activities to some extent.

Compared with our previous report, the number of metabolites found in stomach is larger than that of intestine (Sui et al., 2009). In addition, all metabolites found in intestine are also found in stomach, indicating that they may be carried from stomach to intestine. Overall, in this study and development of orally administrated drug, such as diterpenoid alkaloids, the investigation on their stability and metabolite profiling in stomach should not be overlooked.

Conclusion

A sensitive and specific LC/ESI/MS^n method has been achieved for the general analysis of AC and its metabolites in animal stomach. Elucidation and identification of these metabolites were performed by comparing the protonated molecules, fragmentation pathways and retention times with those obtained from standard compounds and authorized literature works. In the fragmentation pathways of AC-type alkaloids, there are some diagnostic ions, such as $[M+H-18]^+$, $[M+H-60]^+$, $[M+H-60-32-28]^+$ and $[M+H-60-32-28-122]^+/[M+H-60-32-28-138]^+$, which are closely related to specific groups and play an important role in structural identification. AC biotransformation in the stomach occurred mainly by demethylation, hydrolysis, hydroxylation, dehydroxylation and ester-exchange reactions. Among the 14 metabolites, three hydroxylated metabolites have never been reported, and seven lipoaconitines were detected *in vivo* for the first time. The metabolite profiling of AC in stomach suggested that stomach might play an important role in the metabolism of aconitum alkaloids.

Declaration of interest

The authors report no conflicts of interest. The authors alone are responsible for the content and writing of this article.

This work was supported by the 973 Program (Nos 2011CB505300 and 2011CB505305) and the National Natural Sciences Foundation of China (No. 81173507).

References

Borcsa B, Widowitz U, Csupor D, et al. (2011). Semisynthesis and pharmacological investigation of lipo-alkaloids prepared from aconitine. Fitoterapia 82:365–8.

Chan TYK. (2011). Causes and prevention of herb-induced aconite poisonings in Asia. Hum Exp Toxicol 30:2023–6.

Consolini M, Sega M, Zanetti C, et al. (2012). Emulsification of simulated gastric fluids protects wheat alpha-amylase inhibitor 0.19 epitopes from digestion. Food Anal Methods 5:234–43.

Delgado S, Suárez A, Mayo B. (2011). Identification, typing and characterisation of *Propionibacterium* strains from healthy mucosa of the human stomach. Int J Food Microbiol 149:65–72.

Gupta B, Rani M, Salunke R, Kumar R. (2012). In vitro and in vivo studies on degradation of quinalphos in rats. J Hazard Mater 213:285–91.

He F, Dou DQ, Sun Y, et al. (2012). Plasma pharmacokinetics and tissue distribution of arctiin and its main metabolite in rats by HPLC-UV and LC-MS. Planta Med 78:800–6.

Kentaro W, Makoto N, Hideyuki H, et al. (2005). Effects of long-term administrations of aconitine on electrocardiogram and tissue concentrations of aconitine and its metabolites in mice. Forensic Sci Int 148:21–9.

Li N, Cao R, Sui ZG, et al. (2012). Intestinal transport of pure diester-type alkaloids from an aconite extract across the Caco-2 cell monolayer model. Planta Med 78:692–7.

Liu WY, Xu WL, Li P, et al. (2009). Tissue distribution and excretion of baicalein and its main metabolite in rats by LC-MS/MS. J China Pharm Univ 40:348–52.

Pullela R, Young L, Gallagher B, et al. (2008). A case of fatal aconitine poisoning by monkshood ingestion. J Forensic Sci 53:491–4.

Sarti F, Barthelmes J, Iqbal J, et al. (2011). Intestinal enzymatic metabolism of drugs. J Pharm Pharmacol 63:392–9.

Singhuber J, Zhu M, Prinz S, Kopp B. (2009). Aconitum in traditional Chinese medicine – a valuable drug or an unpredictable risk? J Ethnopharmacol 126:18–30.

Strzelecki A, Pichon N, Gaulier JM, et al. (2010). Acute toxic herbal intake in a suicide attempt and fatal refractory ventricular arrhythmia. Basic Clin Pharmacol 107:698–9.

Sui ZG, Jiang YQ, Liu ZQ, et al. (2009). Study on metabolites of aconitine in rabbit intestines by using LC/ESI-MS^n. Acta Chim Sinica 67:2439–44.

Suzuki Y, Oyama T, Ishige A, et al. (1994). Antinociceptive mechanism of the aconitine alkaloids mesaconitine and benzoylmesaconine. Planta Med 60:391–4.

Tang L, Ye L, Chang L, et al. (2011). Involvement of CYP3A4/5 and CYP2D6 in the metabolism of aconitine using human liver microsomes and recombinant CYP450 enzymes. Toxicol Lett 202:47–54.

Turabekova MA, Rasulev BF, Dzhakhangirov FN, Salikhov SI. (2008). Aconitum and delphinium alkaloids: ''drug-likeness'' descriptors related to toxic mode of action. Environ Toxicol Pharmacol 25:310–20.

Wang Y, Liu ZQ, Song FR, Liu SY. (2002). Electrospray ionization tandem mass spectrometry study of the aconitines in the root of aconite. Rapid Commun Mass Spectrom 16:2075–82.

Wang Y, Shi L, Song FR, et al. (2003). Exploring the ester-exchange reactions of diesterditerpenoid alkaloids in the aconite decoction process by electrospray ionization tandem mass spectrometry. Rapid Commun Mass Spectrom 17:279–84.

Wang YG, Wang SQ, Liu YX, et al. (2006). Characterization of metabolites and cytochrome P450 isoforms involved in the microsomal metabolism of aconitine. J Chromatogr B 844:292–300.

Wang ZH, Wen J, He Y. (2004). Research on pharmacokinetic of aconitine by LC-MS. J Instrumental Anal 23:51–6.

Yue H, Pi ZF, Song FR, et al. (2009). Studies on the aconitine-type alkaloids in the roots of *Aconitum Carmichaeli* Debx. by HPLC/ESI/MS/MSn. Talanta 77:1800–7.

Zhang WT, Li Q, Zhu M, et al. (2008). Direct determination of polydatin and its metabolite in rat excrement. Chem Pharm Bull 56:1592–5.

Zhang HG, Sun Y, Duan MY, et al. (2005). Separation and identification of Aconitum alkaloids and their metabolites in human urine. Toxicon 46:500–6.

Zhao YF, Song FR, Guo XH, Liu SY. (2008). Studies on the biotransformation of aconitine in human intestinal bacteria using soft ionization mass spectrometry. Chem J Chin Univ 29:55–9.

Zhao YF, Song FR, Yue H, et al. (2007). Biotransformation of deoxyaconitine of metabolite of aconitine by human intestinal bacteria and electrospray ionization tandem mass spectrometry. Chem J Chin Univ 28:2051–5.

Zhou YP, Liu WH, Zeng GY, et al. (1984). The toxicity of aconitine and its analogs and their effects on cardiac contractile function. Yao Xue Xue Bao 19:641–6.